



Published in final edited form as:

*Angiogenesis*. 2017 November ; 20(4): 479–492. doi:10.1007/s10456-017-9557-6.

## Pathogenic role and therapeutic potential of pleiotrophin in mouse models of ocular vascular disease

Weiwen Wang<sup>1,\*</sup>, Michelle E. LeBlanc<sup>1,\*</sup>, Xiuping Chen<sup>1,3</sup>, Ping Chen<sup>1,4</sup>, Yanli Ji<sup>1,5</sup>, Megan Brewer<sup>1</sup>, Hong Tian<sup>1,6</sup>, Samantha R. Spring<sup>1</sup>, Keith A. Webster<sup>2</sup>, and Wei Li<sup>1,2</sup>

<sup>1</sup>Bascom Palmer Eye Institute, Department of Ophthalmology, University of Miami School of Medicine, Miami, Florida, USA

<sup>2</sup>Vascular Biology Institute, University of Miami School of Medicine, Miami, Florida, USA

<sup>3</sup>Department of Ophthalmology, Zhongshan Hospital of Fudan University, Shanghai, China

<sup>4</sup>Department of Ophthalmology, Renji Hospital of Jiaotong University, Shanghai, China

<sup>5</sup>Department of Ophthalmology, Zhengzhou Eye Hospital, Zhengzhou, Henan, China

<sup>6</sup>School of Public Health, Xinxiang Medical University, Xinxiang, Henan, China

### Abstract

Angiogenic factors play an important role in the pathogenesis of diabetic retinopathy (DR), neovascular age-related macular degeneration (nAMD) and retinopathy of prematurity (ROP). Pleiotrophin, a well-known angiogenic factor, was recently reported to be upregulated in the vitreous fluid of patients with proliferative DR (PDR). However, its pathogenic role and therapeutic potential in ocular vascular diseases have not been defined *in vivo*. Here using corneal pocket assays, we demonstrated that pleiotrophin induced angiogenesis *in vivo*. To investigate the pathological role of pleiotrophin we used neutralizing antibody to block its function in multiple *in vivo* models of ocular vascular diseases. In a mouse model of DR, intravitreal injection of pleiotrophin-neutralizing antibody alleviated diabetic retinal vascular leakage. In a mouse model of oxygen-induced retinopathy (OIR), which is a surrogate model of ROP and PDR, we demonstrated that intravitreal injection of anti-pleiotrophin antibody prevented OIR-induced pathological retinal neovascularization and aberrant vessel tufts. Finally, pleiotrophin-neutralizing antibody ameliorated laser-induced choroidal neovascularization, a mouse model of nAMD, suggesting that pleiotrophin is involved in choroidal vascular disease. These findings suggest that pleiotrophin plays an important role in the pathogenesis of DR with retinal vascular leakage, ROP with retinal neovascularization and nAMD with choroidal neovascularization. The results also support pleiotrophin as a promising target for anti-angiogenic therapy.

---

Correspondence to Wei Li, w.li@med.miami.edu; Tel: +1-305-326-6445; Fax: +1-305-547-3658.

\*These authors contributed equally.

**Author contributions.** W.W., M.E.L., P.C., Y.L., M.B., H.T., S.R.S., performed most of the studies and analyzed data. X.P. carried out corneal pocket assay. M.B. H.T., S.R.S provide supportive experiments. W.L. designed experiments, analyzed data and wrote manuscript. K.W. provided reagents, advised on experimental design and revised manuscript.

Compliance with ethical standards

**Conflict of interest.** The author declare no competing or financial interests.

## Keywords

Pleiotrophin; anti-angiogenic therapy; neovascular age-related macular degeneration; diabetic retinopathy; retinopathy of prematurity; oxygen-induced retinopathy; choroidal neovascularization

---

## Introduction

Angiogenesis plays a pivotal role in ocular vascular disease, including diabetic retinopathy (DR), neovascular age-related macular degeneration (nAMD) and retinopathy of prematurity (ROP). DR, a major cause of vision impairment in working adults, affects ~93 million worldwide [1], including vision-threatening diabetic macular edema (DME) with retinal leakage and proliferative DR (PDR) with retinal neovascularization (RNV). ROP is the most common cause of vision loss in children, affecting ~14,000 – 16,000 preterm infants each year in the U.S. [2]. Similar to PDR, ROP in preterm neonates is characterized by RNV [3]. AMD is the leading cause of blindness in the elderly in developed countries and will afflict an estimated 196 million people worldwide in 2020 [4]. AMD has two clinical forms: dry (atrophic) and wet (neovascular or exudative). nAMD with choroidal neovascularization (CNV) affects 10–20% of individuals with the disease but accounts for about 90% of all cases with severe vision loss from the disease [5].

Angiogenic factors promote ocular neovascularization and vascular leakage. A major breakthrough in the treatment of both nAMD with CNV and DME with vascular leakage was the approval of vascular endothelial growth factor (VEGF) inhibitors, such as Lucentis (ranibizumab) and Eylea (aflibercept) [6, 7]. However, anti-VEGF therapies have limited therapeutic efficacies for both conditions with vision improvement in less than half of patients [8], suggesting the involvement of other angiogenic factors. For example, anti-angiogenic therapy against platelet-derived growth factor (PDGF) is currently in clinical trials for nAMD [9]. The identification and characterization of other angiogenic factors and their therapeutic potential may present novel therapies for nAMD and DME, especially for patients that are unresponsive to anti-VEGF. There is presently no approved drug therapy for PDR without DME. Anti-VEGF therapy has been investigated in a number of clinical trials for ROP, however, efficacy and safety issues have so far precluded its approval [10, 11].

Pleiotrophin (Ptn; also known as HARP, HBGF8, HBNF, NEGF1, Hb-GAM) is a heparin-binding cytokine with diverse functions [12, 13]. Ptn binds to at least five different cell surface receptors, including receptor protein tyrosine phosphatase (RPTP)  $\beta/\zeta$ , tyrosine kinase receptor ALK, N-syndecan,  $\alpha v\beta 3$  integrin and low-density lipoprotein (LDL) receptor-related protein (LRP) [14–19]. Ptn promotes angiogenesis, neurite outgrowth, cell survival, and mitogenesis of fibroblasts [20–22]. A large body of evidence directly implicates Ptn in tumorigenesis by enhancing angiogenesis and proliferation of tumor cells [13, 23]. A recent study suggested that Ptn may be upregulated in the vitreous fluid of PDR patients [21]. However, the pathogenic role and therapeutic potential of Ptn for ocular vascular disease have not been characterized *in vivo*.

Here we investigated the pathogenic role of Ptn in mouse models of ocular vascular disease by blocking its activity with a neutralizing antibody (Ab). Our results suggest that Ptn may

contribute to the pathogenesis of DR, nAMD and ROP and that the blockade of Ptn could be a valuable strategy for anti-angiogenic therapy of these conditions.

## Materials and Methods

### Cell culture

Human retinal microvascular endothelial cells (HRMVECs) and a complete medium kit with fetal bovine serum (FBS) and CultureBoost were purchased from Cell Systems and used for experiments at Passage 4–8 [24].

### Proliferation assay

HRMVECs were seeded in 96-well plates precoated with Attachment Factor (Cell Systems) in the complete medium (Cell Systems) at  $1 \times 10^3$  cells/well. Cells were incubated with Ptn (Sino Biological, Cat. #10288-HNAB-100), VEGF-165 (R&D Systems) or control medium at indicated concentrations. When needed, affinity-purified rabbit anti-Ptn Ab (Proteintech) was washed three times with PBS in Amicon centrifugal filter units (10 kDa cutoff, Millipore) and added to HRMVECs. After culturing for 48 h, cells in each well were collected by trypsin digestion and quantified in PBS with 1 mM trypan blue using a hemocytometer.

### Wound healing assay

HRMVEC migration was analyzed using *in vitro* wound healing assay as described [25, 26]. Briefly, HRMVECs were cultured in 12-well plates until ~90–100% confluence. Cells were starved for 3 h in EBM-2 medium (Lonza) supplemented with 2% FBS. A sterile 200- $\mu$ l tip was used to create a defined and clear scratch approximately 1 mm in width in each well. Dislodged cells were removed by rinsing, and the remaining cells were supplemented with fresh EBM-2 medium containing 2% FBS in the presence of Ptn, VEGF or PBS. The migration of cells was monitored at 0 and 20 h by phase-contrast microscopy. After staining with calcein AM at 20 h, at least 6 images in each well were analyzed by fluorescence microscopy. The percentage of the denuded area covered by migrated cells within the original scratch was quantified using ImageJ software (NIH).

### Transwell migration assay

HRMVEC migration was also quantified using a transwell assay, as described [27]. In brief, HRMVECs ( $2 \times 10^4$  cells/well) were seeded in EBM-2 medium (100  $\mu$ l) supplemented with 2% FBS in the upper chamber of transwell insets (8  $\mu$ m pore) in 24-plates. The same medium was used for the bottom chamber (600  $\mu$ l/well) but supplemented with additional Ptn (200 ng/ml), VEGF (50 ng/ml) or PBS. After 8 h in culture, the membranes were washed with PBS, fixed with 4% formaldehyde. After wiping cells off the upper side of the membrane with a cotton swab, the membranes were detached, stained with DAPI, mounted on slides and quantified by fluorescence microscopy.

### Endothelial spheroid sprouting assay

The assay was performed with HRMVECs as described [26]. Briefly, HRMVECs at 80% confluence were harvested, counted, resuspended in EBM-2 medium containing 20% methocel and 10% FBS, seeded at 750 cells/well in non-adhesive 96-well round-bottomed plates and cultured for 24 h. Methocel solution was prepared by dissolving methycellulose (Sigma) in EBM-2 medium at 1.2% and centrifuged at  $5,000 \times g$  for 2 h at 4°C to clear debris. Spheroids were harvested, resuspended in EBM-2 medium containing fibrinogen (2.5 mg/ml) and aprotinin (0.05 mg/ml), and seeded in 24-well plates (~50 spheroids/ml/well). Clotting was induced by adding thrombin (12 units/ml) to each well. The spheroid-embedded fibrin gel was allowed to clot for 5 min at room temperature and then 20 min at 37°C. The fibrin gel was equilibrated with 1 ml of EBM-2 medium containing aprotinin (0.05 mg/ml) in the presence of Ptn, VEGF or PBS, and incubated for 48 h at 37°C. Photographs were taken using a phase contrast microscope, and average sprout lengths were quantified using ImageJ.

### Kinase activation

The activation of ERK1/2 and Akt was detected by Western blot as described [26]. Briefly, HRMVECs were seeded in 6-well plates precoated with Attachment Factor (Cell Systems) and cultured to ~90% confluence. Cells were preincubated in EBM-2 medium for 15 min  $\times$  3 times at 37°C to reduce the effect of other growth factors. Cells were incubated with Ptn, VEGF or PBS for 10 or 30 min in 37°C and lysed in RIPA buffer (Pierce Biotechnology) containing phosphatase inhibitor cocktail (Roche). Lysates were analyzed by Western blot using Ab against phosphorylated ERK1/2 (pEKR1/2), total ERK1/2, phosphorylated Akt (pAkt, Thr308), total Akt or  $\beta$ -actin (Cell Signaling), followed by horseradish peroxidase-labeled secondary Ab for chemiluminescence signal detection.

### Corneal pocket assay

The assay was carried out as described [26]. Briefly, sterilized Whatman filter paper (Grade 3) (GE Healthcare Bio-Sciences) was cut into pieces (0.125 mm<sup>2</sup>/piece). The paper was soaked in the solution of Ptn, VEGF or PBS for 2 h at 4°C, and implanted into corneal pockets of anesthetized C57BL/6 mice (8–10 weeks old; 1 paper/cornea; 2 pockets/mouse). After 6 days, angiogenesis in each eye was evaluated using a slit-lamp microscope and photographed. The numbers of new sprouting vessels into the cornea and their branching points were quantified. In addition, we semiquantitatively analyzed the number, density, length of visible corneal blood vessels with a comprehensive scoring system [26]. Mice were then euthanized by CO<sub>2</sub>, and immediately perfused intracardially with lipophilic fluorescent DiI dye to label blood vessels. Eyes were removed and fixed in 10% formalin for 24 h at 4°C. Corneas were dissected right at the limbus, flat-mounted in 50% glycerol/PBS, and imaged by confocal microscopy to detect DiI-labeled blood vessels.

All animal procedures in this study were approved by the Institutional Animal Care and Use Committee at the University of Miami and complied with the *Guide for the Care and Use of Laboratory Animals* published by the United States NIH.

### Diabetic retinal vascular leakage

C57BL/6 mice (6–7 weeks old) were intraperitoneally treated with streptozotocin (STZ) (starving for 4 h, followed by 50 µg/g body weight, for 5 consecutive days) or mock citrate buffer. Blood glucose was monitored biweekly. Hyperglycemic mice with blood glucose 350 mg/dL were aged for 4 months to develop retinal vascular leakage. Anti-Ptn Ab, control rabbit IgG or aflibercept was intravitreally injected into 4-month-diabetic mice. PBS was injected into fellow eyes. Retinal vascular leakage in diabetic mice was quantified by Evans blue assay [24, 28]. Briefly, Evans blue (0.15 mg/g body weight) was intravenously injected 1.5 h post intravitreal injection. Mice were intracardially perfused with pre-warmed (37°C) sodium citrate buffer (100 mM, pH 4.5) 2.5 h post Evans blue injection. Prior to perfusion, blood was collected via a cardiac punch. After perfusion, retinas were isolated and incubated in formamide (50 µl/retina) overnight at 70°C to extract Evans blue dye from the retina. The solution was centrifuged at 128,000 g at 4°C for 45 min. Evans blue in the supernatant was quantified spectrometrically at 620 nm and 740 nm (background) and compared to a standard curve. The blood samples were centrifuged at 3,550 g for 15 min at 25°C, diluted and quantified at the same wavelengths. Evans blue was calculated using the following formula: [leaked Evans blue concentration (mg/ml)/retinal weight (mg)]/[blood Evans blue concentration (mg/ml) × circulation time (h)].

### OIR

OIR was performed as previously described [24, 29]. C57BL/6 mice at postnatal day 7 (P7) and their nursing mothers were exposed to 75% oxygen in a regulated chamber for 5 days. At P12, Ptn Ab, aflibercept or control IgG was intravitreally injected into anesthetized mice. PBS was injected into fellow eyes. Mice were returned to room air after injection. At P17 mice were euthanized by CO<sub>2</sub> inhalation. After fixation of enucleated eyes with 4% paraformaldehyde, retinas were isolated and stained with Alexa Fluor 488-isolectin B4, flat-mounted and analyzed by confocal microscopy. Neovascularization and avascular area were quantified using Photoshop [29]. Additionally, the number of neovascularization tufts and branching points was counted.

### CNV

C57BL/6 mice (7–8 weeks old) were subjected to laser photocoagulation (Argon laser, 532 nm, 100 mW, 100 ms, 100 µm, 4 spots/retina around the optic disc) on Day 0, as described [24]. Lesions were confirmed by subretinal bubbles developed immediately after laser treatment. Additionally, CNV was verified by spectral domain-optical coherence tomography (SD-OCT) [24]. Lesions with choroidal hemorrhage and linear or fused lesions were excluded as described [30]. Mice received intravitreal injection of anti-Ptn Ab, aflibercept or control IgG on Day 3. PBS was injected into fellow eyes. CNV lesions were analyzed by fluorescein angiography on Day 7. Briefly, fluorescein sodium (2.5%, 0.1 mL, Akorn) was intraperitoneally injected into mice [24, 31]. Fluorescein angiography was performed 6 min post injection using Heidelberg Engineering Multiline HRA SN 2884 Imaging System. CNV leakage (i.e., leaked fluorescence intensity) was quantified as pixel intensity using Photoshop.

Mice were euthanized on Day 8 by CO<sub>2</sub> inhalation. Eyecups of the retinal pigment epithelium (RPE)-choroid-sclera were isolated and fixed in 4% paraformaldehyde. Eyecups were incubated in PBS containing 0.5% Triton X-100 at 4°C for 24 h and stained with Alexa Fluor 488-isolectin B4 (10 µg/ml, 0.5 ml/retina) overnight at room temperature [24, 31]. After washing, eyecups were flat mounted and analyzed by confocal microscopy. Z-stack images were deconvoluted to build a 3D image and quantified for the volume of the CNV lesions (Volocity software). Additionally, the largest CNV z-stack image of each lesion was quantified to determine the CNV area using ImageJ. CNV vessel density was determined by quantifying the pixel threshold intensity of each CNV lesion using the Magic Wand Tool in Adobe Photoshop CSS Extended software.

### Statistical analysis

Data were expressed as mean ± s.e.m. and analyzed by Student's t-test or one-way ANOVA test. Data were considered significant when  $p < 0.05$ .

## Results

### Ptn stimulates retinal endothelial proliferation

As a first step to define putative pro-angiogenic roles for Ptn in ocular disease, we measured the proliferation rates of HRMVECs cultured in the presence or absence of Ptn or VEGF. Ptn significantly induced the growth of HRMVECs in a dose-dependent manner (Fig. 1A). As a positive control, VEGF (50 ng/ml) also significantly stimulated HRMVEC proliferation. These results confirm that Ptn is mitogenic for retinal endothelial cells.

### Ptn promotes endothelial cell migration

Endothelial cell migration is an integral part of angiogenesis process. Therefore, we analyzed the activity of Ptn to induce the migration of HRMVECs by performing *in vitro* wound healing assays. The results indicated that Ptn at 200 ng/ml significantly facilitated endothelial migration ( $p < 0.05$ , Fig. 1B, C). As a positive control, VEGF (50 ng/ml) induced a similar pattern of endothelial migration ( $p < 0.01$ ). Transwell migration assay independently corroborated that Ptn and VEGF stimulated the migration of HRMVECs (Fig. 1D, E). These data indicate that Ptn is an angiogenic factor capable of promoting the migration of retinal endothelial cells.

### Ptn induces spheroid sprouting of endothelial cells

Spheroid sprouting assays provide an *in vitro* 3D model to analyze the activity of angiogenic factors. We quantified the angiogenic activity of Ptn by performing the assay with HRMVECs. Quantification of average length of endothelial sprouts indicated that Ptn at 20 ng/ml significantly stimulated spheroid sprouting of HRMVECs ( $p < 0.0001$ , Fig. 2). VEGF (5 ng/ml) as a positive control promoted similar endothelial sprouting ( $p < 0.001$ ).

### Ptn activates ERK and Akt

Previous studies have reported that Ptn induces the activation of extracellular signal-regulated kinase 1/2 (ERK1/2) and Akt [21, 32]. However, one study showed that Ptn



inhibits endogenous Akt activity in cardiomyocytes [33]. We analyzed Ptn-induced activation of the kinases in HRMVECs. As shown in Fig. 3, we found that Ptn induced the phosphorylation of both ERK1/2 and Akt. As a positive control, VEGF stimulated similar kinase activations.

### **Ptn is an angiogenic factor *in vivo***

To verify Ptn as an angiogenic factor *in vivo*, we performed corneal pocket assay in mice. The results showed that Ptn induced corneal angiogenesis, as detected by slit-lamp microscopy (Fig. 4A). This finding was independently verified by staining corneal blood vessels with fluorescent DiI dye (Fig. 4B). Quantification of new corneal vessels and their branching points revealed that Ptn significantly stimulated corneal angiogenesis ( $p < 0.01$ , Fig. 4C,D). Furthermore, quantification of a comprehensive score for the number, density and length of visible corneal blood vessels [26] showed that Ptn significantly induced corneal angiogenesis ( $p < 0.01$ , Fig. 4E). As a positive control, VEGF also significantly promoted corneal angiogenesis according to all these three methods of quantification ( $p < 0.001$ ). These *in vivo* results are consistent with previous findings that Ptn is an angiogenic factor [34].

### **Anti-Ptn therapy alleviates diabetic retinal vascular leakage**

Selective upregulation of Ptn in the vitreous of PDR patients suggests an association with DR pathogenesis [21]. However, such association has not been demonstrated directly. Therefore we used an affinity-purified Ab to neutralize Ptn activity in mouse models of DR. The specificity of anti-Ptn Ab was analyzed by Western blot using mouse retina. The results showed that Ptn Ab specifically recognized Ptn but not other retinal proteins (Fig. 5A). The neutralizing activity of affinity-purified anti-Ptn Ab was demonstrated using an endothelial proliferation assay. The results confirmed that Ptn Ab inhibited Ptn- but not VEGF-induced HRMVEC proliferation ( $p < 0.01$ , Fig. 5B).

DME with retinal vascular leakage is a major vision-threatening condition of DR. Angiogenic factors play an important role in diabetic vascular leakage [35], as evidenced by the success of anti-VEGF therapy of DME [6]. Diabetes was induced in mice with STZ as described in Methods, and hyperglycemic mice were aged for 4 months to develop DR. Retinal vascular leakage in 4-month-diabetic mice was verified by Evans blue assay ( $p < 0.01$ , Fig. 6A). Intravitreal injection of Ptn-neutralizing Ab alleviated retinal vascular leakage in diabetic mice ( $p < 0.01$ , Fig. 6B). As a positive control, the VEGF inhibitor aflibercept also reduced diabetic vascular leakage with similar efficacy ( $p < 0.01$ , Fig. 6B). These results suggest that Ptn is an important angiogenic factors in DR pathogenesis and a possible target for DME therapy.

### **Anti-Ptn therapy inhibits OIR-induced neovascularization**

Diabetic patients usually develop PDR with RNV 15–20 years after diabetes onset. In contrast, diabetic rodents rarely develop PDR, possibly due to their short lifespan. Oxygen-induced retinopathy (OIR) with RNV is an alternate animal model of ROP that has been widely used as a surrogate model of PDR [36, 37]. To create this model, neonatal mice were exposed to hyperoxia to induce vascular regression. As shown in Fig. 7, an avascular region

was observed to form in the central retina of OIR mice, as expected. Subsequent exposure to normoxia induced pathological RNV and neovascular tufts in the peripheral retina (Fig. 7). Compared to the healthy retina, OIR retina showed disorganized vascular structure (Fig. 7A, zoom-in, 1 vs. 2 or 3). This phenotype of OIR is consistent with previous studies [29].

Intravitreal injection of anti-Ptn Ab immediately before exposure to normoxia prevented RNV and neovascular tuft formation (Fig. 7A). Quantification of vessel density and neovascularization tufts showed that Ptn Ab significantly prevented OIR-induced pathological RNV and aberrant vessel tufts ( $p < 0.05$ , Fig. 7B, C). It is worth noting that anti-Ptn Ab restored the structural integrity of retinal vasculature (Fig. 7A, zoom-in, 5 vs. 2 or 3). Indeed, quantification of vessel branching points, characteristic of the phenotypes of neovascularization, indicated that Ptn-neutralizing Ab significantly inhibited OIR-induced vessel branching ( $p < 0.01$ , Fig. 7D). As a positive control, aflibercept reduced RNV, neovascular tufts and vessel branching with similar efficacies. However, the avascular area in the central retina was unaffected by either Ptn Ab or aflibercept ( $p > 0.05$  for all groups vs. PBS, Fig. 7E). These results suggest that Ptn contributes to the pathogenesis of OIR and is a potential target for the therapy of ROP and PDR.

### Anti-Ptn therapy ameliorates laser-induced CNV

Laser-induced CNV is a widely used animal model of nAMD. To quantify the effect of anti-Ptn Ab, we analyzed CNV lesion by two different methods: fluorescein angiography and histological examination of CNV. Intravitreal injection of anti-Ptn Ab significantly reduced vascular leakage of laser-induced CNV lesions as detected by fluorescein angiography ( $p < 0.05$ , Fig. 8A, B). As a positive control, aflibercept also inhibited CNV leakage with similar efficacy in this model ( $p < 0.05$ ). Histological analysis of CNV lesion was performed by labeling CNV vessels with Alexa Fluor 488-isolectin B4 (Fig. 8C). Quantification of CNV 3D volume indicated that Ptn-neutralizing Ab significantly alleviated laser-induced CNV ( $p < 0.01$ , Fig. 8D). Additionally, the area size and vessel density (i.e., fluorescence pixel intensity) of CNV were inhibited by anti-Ptn Ab ( $p < 0.01$ , Fig. 8E, F). Similarly, aflibercept also significantly reduced the volume, area size and vessel density of CNV (Fig. 8C–F). These data suggest that Ptn is an important angiogenic factor in the pathogenesis of laser-induced CNV and a promising target for anti-angiogenic therapy of nAMD.

## Discussion

Our results confirm pro-angiogenic and vascular permeability actions of Ptn in multiple mouse models of ocular disease and provide the first evidence that Ptn may be an important target for Ab therapy as a sole agent or possibly in combination with other anti-angiogenic Abs. We found that anti-Ptn Ab alleviated retinal vascular leakage in DR mice, pathological RNV in OIR mice and CNV in laser-treated mice.

Ptn is well recognized for its activity to promote neurite outgrowth [22]. However, its mitogenic activity is controversial [20, 38, 39]. It was suggested that Ptn produced in a mammalian system, but not in insect cells or bacteria, was capable of stimulating endothelial proliferation [40]. However, a previous study showed that Ptn expressed and purified from bacteria enhanced the proliferation and migration of microglial cells [41]. Another study



showed that Ptn produced in bacteria moderately promoted HUVEC proliferation, albeit not statistically significant [40]. Ptn in this study was expressed and purified in insect cells. We found that this Ptn can stimulate the proliferation, migration, and spheroid sprouting of HRMVECs with statistical significance (Fig. 1, 2). This was independently verified by Ptn-induced ERK and Akt activation (Fig. 3). However, Ptn activities were detected at much higher concentrations than VEGF in all these assays.

Ptn and midkine (MK) form a distinct family of heparin-binding growth factors with sequence homology [42]. Ptn is highly conserved with more than 90% sequence identity across different species [43]. Ptn is a cytokine with diverse biological functions, including differentiation of oligodendrocyte progenitor cells, neurite outgrowth, axonal remyelination and angiogenesis [22, 23, 44]. Ptn is a mitogen for endothelial cells, epithelial cells and fibroblast cells [20, 39, 45], and is expressed in multiple cancers, including breast, prostate, ovarian, lung, melanoma, head and neck, glioblastoma, neuroblastoma, pancreatic carcinoma and choriocarcinoma [13]. The cytokine is a prognostic factor for colorectal cancer [46] and a protooncogene associated with tumor angiogenesis and tumor cell proliferation [47]. *In vitro* functional assays, including tube formation, migration and sprouting of endothelial cells from various organs, confirm a direct angiogenic activity of Ptn [21, 48]. *In vivo* angiogenic activity of Ptn has also been confirmed in Ptn-overexpressing tumor cells. For example, Ptn-expressing NIH 3T3 cells formed tumors in nude mice with significant neovascularization [47]. Overexpression of Ptn in human adrenal carcinoma cells promoted tumor growth with a striking increase in the density of new blood vessels [49]. Our studies are consistent with this and further demonstrate similar angiogenic activity of Ptn in a tumor-free setting in the corneal pocket assay (Fig. 4). The results suggest that Ptn drives angiogenesis *in vivo* in tumor- and non-tumor settings.

It was recently reported that Ptn was elevated in the vitreous fluid of PDR patients, suggesting a possible role in PDR disease progression [21]. Our results provide direct support for such an interpretation. We found that Ptn induced the proliferation, migration and spheroid sprouting of HRMVECs (Fig. 1, 2). Consistent with angiogenic stimulation, Ptn activated the key angiogenic signaling pathways ERK1/2 and Akt with responses similar to those of VEGF (Fig. 3) [50]. Ptn binds to at least five different cell surface receptors, including RPTP $\beta$ / $\zeta$ , ALK and  $\alpha$ v $\beta$ 3 integrin [14–18]. Some of these receptors, including ALK and integrin, are known to activate ERK and Akt [51, 52]. Different subcellular locations of activated ERK may lead to distinct cellular responses [53]. Because Ptn and VEGF have distinct receptor signaling pathways they may also drive different pathways of angiogenesis. Such distinct mechanisms of action provide a possible a molecular basis for anti-Ptn as an alternative anti-angiogenic therapy.

Results from our mouse models (Fig. 7–8) strongly implicate Ptn as an angiogenic factor in the pathogenesis of ocular neovascular diseases, including ROP and nAMD. The high efficacy of anti-Ptn Ab to suppress angiogenesis during OIR suggests that Ptn contributes importantly to the pathogenesis of ROP and PDR. Similarly, the high efficacy of anti-Ptn therapy to alleviate CNV implicates Ptn in nAMD.

It is well known that VEGF confers vascular permeability as well as angiogenesis by disrupting endothelial tight junctions [54, 55], and retinal vascular leakage is a hallmark of most ocular angiogenic diseases, including nAMD and PDR. By using fluorescein angiography, we demonstrated that anti-Ptn Ab, like anti-VEGF, markedly alleviated diabetic retinal vascular leakage in STZ-treated mice (Fig. 6B) in the absence of RNV. This suggests that Ptn may stimulate DR leakage without triggering angiogenesis.

Interestingly, a previous study reported that aflibercept increased the avascular area in OIR mice [56]. However, we found no enlargement of the avascular region by either Ptn Ab or aflibercept (Fig. 7E). The variation between these two studies may be attributed to differences in the OIR timeline and doses of aflibercept. The previous study showed that aflibercept in a relatively high dose further expanded the avascular region [56]. One possible explanation is that the dose of aflibercept in our study is slightly lower than that of the previous report.

Previous studies suggest that Ptn interacts with VEGF to either promote or suppress angiogenesis. For example, Ptn induces VEGF expression to promote angiogenesis [21, 46, 57]. On the other hand, Ptn directly binds to VEGF and inhibits VEGF-induced endothelial proliferation and tube formation [58]. Another group reported that VEGF bound to RPTP $\beta$ / $\zeta$  and that Ptn interrupted this binding to inhibit VEGF-induced endothelial migration [59, 60]. Additionally, Ptn suppressed the expression of VEGF receptor 2 (VEGFR2), thereby inhibiting VEGF-induced endothelial proliferation and migration [61]. Instead of investigating how all these interactions may modulate Ptn angiogenic activity in various assay models, we analyzed if Ptn plays a detrimental or protective role in different retinal vascular diseases in *in vivo* settings. Our data showed that inhibition of Ptn alleviated DR leakage, OIR-induced RNV and laser-induced CNV (Fig. 6B–8). These results suggest that pro-angiogenic activity of Ptn contributes to the pathogenesis of these retinal vascular diseases. However, it is difficult to determine if Ptn regulates angiogenesis directly or indirectly and what percentage of pathogenic contribution these direct and indirect pathways may have. Future studies should be channeled towards the investigation of which Ptn receptors are involved in retinal vascular diseases for possible receptor-specific blockade.

Taken together our findings suggest that Ptn is a target for anti-angiogenic therapy of nAMD, DME, PDR and ROP. This is particularly important for ROP, for which there is no approved pharmacological therapy. Because Ptn is a cytokine that regulates the function of a broad spectrum of cells, including neurons, glial cells and epithelial cells [12], systemic blockade may have side effects by affecting normal cell physiology. Similarly, VEGF is a broad-spectrum cytokine, known to regulate normal endothelial cells, neurons, retinal pigment epithelium and many other cells [62–64]. Nonetheless, intravitreal anti-VEGF therapy for DME and nAMD appears to be safe and well-tolerated in patients. Interestingly, our recent comparative ligandomics analysis revealed that Ptn selectively bound to diabetic but not healthy retinal vessels (38:0 for diabetic:control), even though this disease selectivity is much less than secretogranin III (Scg3) (1,731:0) [65]. This binding selectivity implicates that anti-Ptn may have minimal side effects on normal vessels. Therefore it seems possible that intravitreal anti-Ptn will also have a safety profile either as sole therapy or in combination with other anti-angiogenic agents, including anti-VEGF. From their work on

breast tumors, Lynn et al. [66] recently postulated that the combination of anti-VEGF and anti-Ptn Abs may provide optimal anti-tumor therapy to block angiogenesis and improve the immunogenicity of tumor cells. Such combinations may also be beneficial for angiogenic ocular diseases, and it will be important to characterize dose, efficacy and safety of sole agent and combination treatments in multiple disease models as preliminary to clinical testing. It should be noted that because of the limited efficacy of currently approved anti-VEGF therapy, ocular diseases and related blindness remain urgent unmet clinical needs.

In summary, this study found that Ptn plays an important role in the pathogenesis of diabetic retinal vascular leakage, OIR-induced RNV and laser-induced CNV. These results suggest that Ptn is a potential target for anti-angiogenic therapy of DME, PDR, ROP and nAMD.

## Acknowledgments

We thank F. Zhang and R. Wen for instrument support; G. Gaidosh for confocal service.

**Funding.** This work was supported by NIH R01GM094449 (W.L.), R21HD075372 (W.L.), R21EY027065 (W.L.), Special Scholar Award from Research to Prevent Blindness (RPB) (W.L.), American Heart Association Predoctoral Fellowship 14PRE18310014 (M.E.L) and 16PRE27250308 (M.E.L), NIH P30-EY014801 and an institutional grant from RPB.

## References

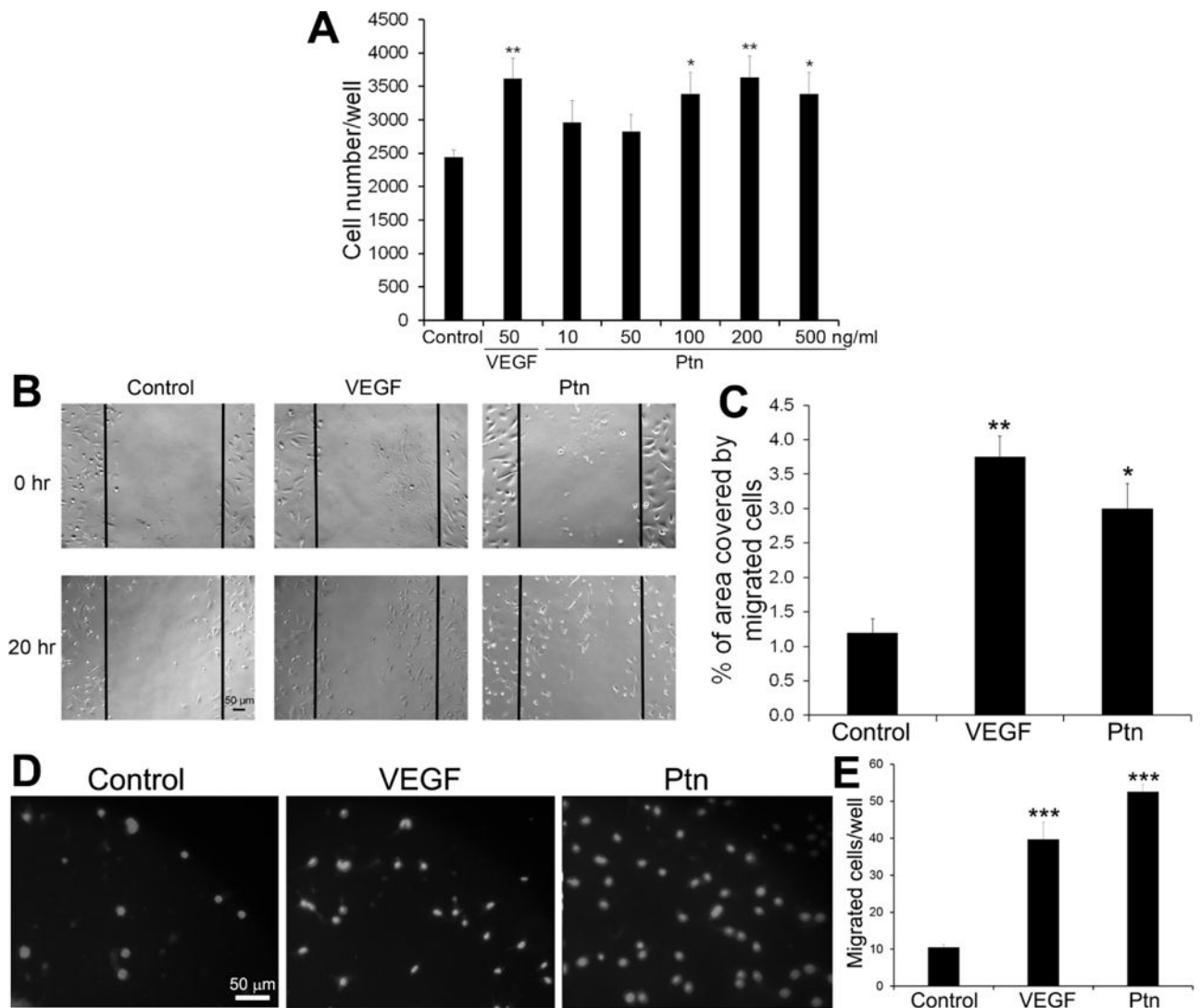
1. Yau JW, Rogers SL, Kawasaki R, Lamoureux EL, Kowalski JW, Bek T, et al. Global prevalence and major risk factors of diabetic retinopathy. *Diabetes care*. 2012; 35(3):556–64. [PubMed: 22301125]
2. Beharry KD, Valencia GB, Lazzaro DR, Aranda JV. Pharmacologic interventions for the prevention and treatment of retinopathy of prematurity. *Semin Perinatol*. 2016; 40(3):189–202. [PubMed: 26831641]
3. Hellstrom A, Smith LE, Dammann O. Retinopathy of prematurity. *Lancet*. 2013; 382(9902):1445–57. [PubMed: 23782686]
4. Wong WL, Su X, Li X, Cheung CM, Klein R, Cheng CY, et al. Global prevalence of age-related macular degeneration and disease burden projection for 2020 and 2040: a systematic review and meta-analysis. *Lancet Glob Health*. 2014; 2(2):e106–16. [PubMed: 25104651]
5. Votruba M, Gregor Z. Neovascular age-related macular degeneration: present and future treatment options. *Eye (Lond)*. 2001; 15(Pt 3):424–9. [PubMed: 11450768]
6. Diabetic Retinopathy Clinical Research Network. Wells JA, Glassman AR, Ayala AR, Jampol LM, Aiello LP, et al. Aflibercept, bevacizumab, or ranibizumab for diabetic macular edema. *N Engl J Med*. 2015; 372(13):1193–203. [PubMed: 25692915]
7. Kim LA, D'Amore PA. A brief history of anti-VEGF for the treatment of ocular angiogenesis. *Am J Pathol*. 2012; 181(2):376–9. [PubMed: 22749677]
8. Dedania VS, Bakri SJ. Current perspectives on ranibizumab. *Clin Ophthalmol*. 2015; 9:533–42. [PubMed: 25848203]
9. Drolet DW, Green LS, Gold L, Janjic N. Fit for the Eye: Aptamers in Ocular Disorders. *Nucleic Acid Ther*. 2016; 26(3):127–46. [PubMed: 26757406]
10. Mintz-Hittner HA, Kennedy KA, Chuang AZ, Group B-RC. Efficacy of intravitreal bevacizumab for stage 3+ retinopathy of prematurity. *N Engl J Med*. 2011; 364(7):603–15. [PubMed: 21323540]
11. Lepore D, Quinn GE, Molle F, Baldascino A, Orazi L, Sammartino M, et al. Intravitreal bevacizumab versus laser treatment in type 1 retinopathy of prematurity: report on fluorescein angiographic findings. *Ophthalmology*. 2014; 121(11):2212–9. [PubMed: 25001158]
12. Deuel TF, Zhang N, Yeh HJ, Silos-Santiago I, Wang ZY. Pleiotrophin: a cytokine with diverse functions and a novel signaling pathway. *Arch Biochem Biophys*. 2002; 397(2):162–71. [PubMed: 11795867]

13. Papadimitriou E, Mikelis C, Lampropoulou E, Koutsoumpa M, Theochari K, Tsirmoula S, et al. Roles of pleiotrophin in tumor growth and angiogenesis. *Eur Cytokine Netw.* 2009; 20(4):180–90. [PubMed: 20167557]
14. Raulo E, Chernousov MA, Carey DJ, Nolo R, Rauvala H. Isolation of a neuronal cell surface receptor of heparin binding growth-associated molecule (HB-GAM). Identification as N-syndecan (syndecan-3). *J Biol Chem.* 1994; 269(17):12999–3004. [PubMed: 8175719]
15. Bernard-Pierrot I, Delbe J, Rouet V, Vigny M, Kerros ME, Caruelle D, et al. Dominant negative effectors of heparin affinity regulatory peptide (HARP) angiogenic and transforming activities. *J Biol Chem.* 2002; 277(35):32071–7. [PubMed: 12070152]
16. Bermek O, Diamantopoulou Z, Polykratis A, Dos Santos C, Hama-Kourbali Y, Burlina F, et al. A basic peptide derived from the HARP C-terminus inhibits anchorage-independent growth of DU145 prostate cancer cells. *Exp Cell Res.* 2007; 313(19):4041–50. [PubMed: 17727841]
17. Mikelis C, Sfaelou E, Koutsoumpa M, Kieffer N, Papadimitriou E. Integrin alpha(v)beta(3) is a pleiotrophin receptor required for pleiotrophin-induced endothelial cell migration through receptor protein tyrosine phosphatase beta/zeta. *FASEB J.* 2009; 23(5):1459–69. [PubMed: 19141530]
18. Kadomatsu K, Muramatsu T. Midkine and pleiotrophin in neural development and cancer. *Cancer letters.* 2004; 204(2):127–43. [PubMed: 15013213]
19. Meng K, Rodriguez-Pena A, Dimitrov T, Chen W, Yamin M, Noda M, et al. Pleiotrophin signals increased tyrosine phosphorylation of beta catenin through inactivation of the intrinsic catalytic activity of the receptor-type protein tyrosine phosphatase beta/zeta. *Proc Natl Acad Sci U S A.* 2000; 97(6):2603–8. [PubMed: 10706604]
20. Fang W, Hartmann N, Chow DT, Riegel AT, Wellstein A. Pleiotrophin stimulates fibroblasts and endothelial and epithelial cells and is expressed in human cancer. *J Biol Chem.* 1992; 267(36):25889–97. [PubMed: 1464602]
21. Zhu X, Bai Y, Yu W, Pan C, Jin E, Song D, et al. The effects of pleiotrophin in proliferative diabetic retinopathy. *PLoS One.* 2015; 10(1):e0115523. [PubMed: 25617851]
22. Rauvala H. An 18-kd heparin-binding protein of developing brain that is distinct from fibroblast growth factors. *EMBO J.* 1989; 8(10):2933–41. [PubMed: 2583087]
23. Perez-Pinera P, Berenson JR, Deuel TF. Pleiotrophin, a multifunctional angiogenic factor: mechanisms and pathways in normal and pathological angiogenesis. *Curr Opin Hematol.* 2008; 15(3):210–4. [PubMed: 18391787]
24. LeBlanc ME, Wang W, Chen X, Ji Y, Shakya A, Shen C, et al. The regulatory role of hepatoma-derived growth factor as an angiogenic factor in the eye. *Mol Vis.* 2016; 22:374–86. [PubMed: 27122967]
25. Liang CC, Park AY, Guan JL. In vitro scratch assay: a convenient and inexpensive method for analysis of cell migration in vitro. *Nat Protoc.* 2007; 2(2):329–33. [PubMed: 17406593]
26. LeBlanc ME, Wang W, Caberoy NB, Chen X, Guo F, Alvarado G, et al. Hepatoma-derived growth factor-related protein-3 is a novel angiogenic factor. *PLoS One.* 2015; 10(5):e0127904. [PubMed: 25996149]
27. Heiss C, Wong ML, Block VI, Lao D, Real WM, Yeghiazarians Y, et al. Pleiotrophin induces nitric oxide dependent migration of endothelial progenitor cells. *J Cell Physiol.* 2008; 215(2):366–73. [PubMed: 17960557]
28. Schepke L, Aguilar E, Gariano RF, Jacobson R, Hood J, Doukas J, et al. Retinal vascular permeability suppression by topical application of a novel VEGFR2/Src kinase inhibitor in mice and rabbits. *J Clin Invest.* 2008; 118(6):2337–46. [PubMed: 18483622]
29. Connor KM, Krahn NM, Dennison RJ, Aderman CM, Chen J, Guerin KI, et al. Quantification of oxygen-induced retinopathy in the mouse: a model of vessel loss, vessel regrowth and pathological angiogenesis. *Nat Protoc.* 2009; 4(11):1565–73. [PubMed: 19816419]
30. Poor SH, Qiu Y, Fassbender ES, Shen S, Woolfenden A, Delpero A, et al. Reliability of the mouse model of choroidal neovascularization induced by laser photocoagulation. *Invest Ophthalmol Vis Sci.* 2014; 55(10):6525–34. [PubMed: 25205860]
31. Chan N, He S, Spee CK, Ishikawa K, Hinton DR. Attenuation of choroidal neovascularization by histone deacetylase inhibitor. *PLoS One.* 2015; 10(3):e0120587. [PubMed: 25807249]

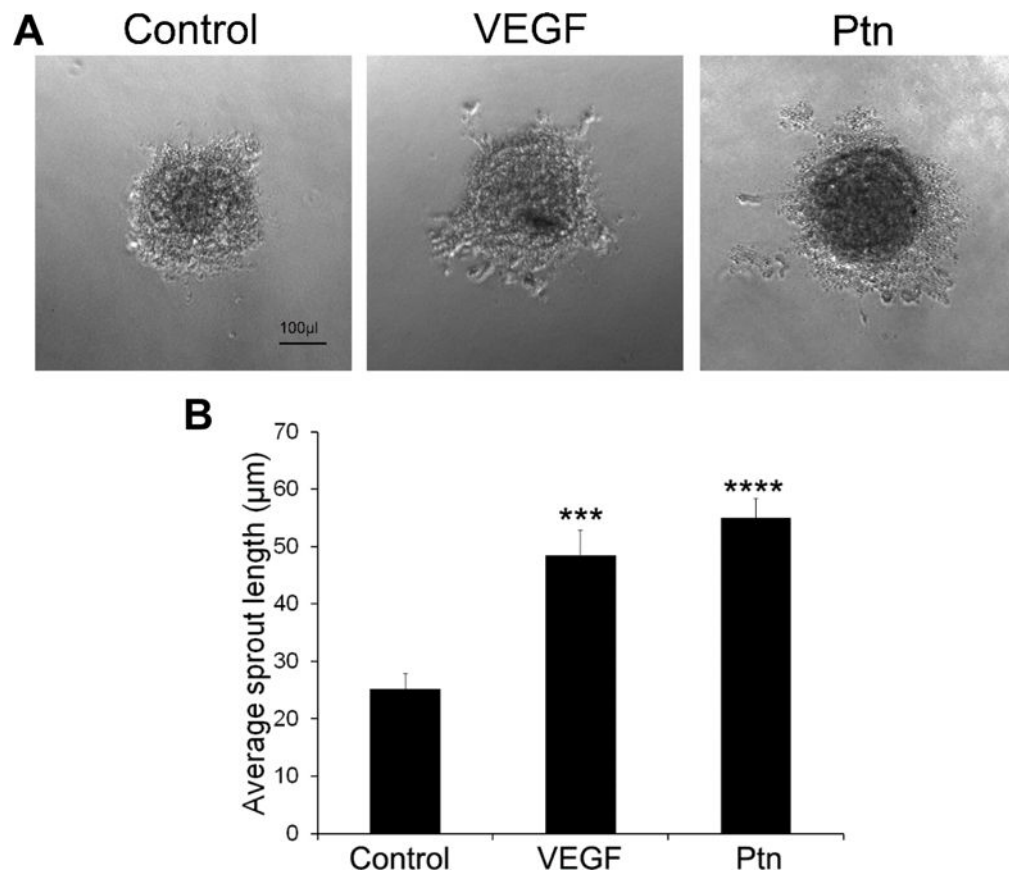
32. Fan JB, Liu W, Yuan K, Zhu XH, Xu DW, Chen JJ, et al. EGFR trans-activation mediates pleiotrophin-induced activation of Akt and Erk in cultured osteoblasts. *Biochem Biophys Res Commun.* 2014; 447(3):425–30. [PubMed: 24727451]
33. Li J, Wei H, Chesley A, Moon C, Krawczyk M, Volkova M, et al. The pro-angiogenic cytokine pleiotrophin potentiates cardiomyocyte apoptosis through inhibition of endogenous AKT/PKB activity. *J Biol Chem.* 2007; 282(48):34984–93. [PubMed: 17925408]
34. Choudhuri R, Zhang HT, Donnini S, Ziche M, Bicknell R. An angiogenic role for the neurokines midkine and pleiotrophin in tumorigenesis. *Cancer research.* 1997; 57(9):1814–9. [PubMed: 9135027]
35. Rask-Madsen C, King GL. Vascular complications of diabetes: mechanisms of injury and protective factors. *Cell Metab.* 2013; 17(1):20–33. [PubMed: 23312281]
36. Stahl A, Connor KM, Sapieha P, Chen J, Dennison RJ, Krah NM, et al. The mouse retina as an angiogenesis model. *Invest Ophthalmol Vis Sci.* 2010; 51(6):2813–26. [PubMed: 20484600]
37. Kim CB, D'Amore PA, Connor KM. Revisiting the mouse model of oxygen-induced retinopathy. *Eye Brain.* 2016; 8:67–79. [PubMed: 27499653]
38. Raulo E, Julkunen I, Merenmies J, Pihlaskari R, Rauvala H. Secretion and biological activities of heparin-binding growth-associated molecule. Neurite outgrowth-promoting and mitogenic actions of the recombinant and tissue-derived protein. *J Biol Chem.* 1992; 267(16):11408–16. [PubMed: 1597470]
39. Delbe J, Vacherot F, Laaroubi K, Barritault D, Courty J. Effect of heparin on bovine epithelial lens cell proliferation induced by heparin affinity regulatory peptide. *J Cell Physiol.* 1995; 164(1):47–54. [PubMed: 7790396]
40. Papadimitriou E, Heroult M, Courty J, Polykratis A, Stergiou C, Katsoris P. Endothelial cell proliferation induced by HARP: implication of N or C terminal peptides. *Biochem Biophys Res Commun.* 2000; 274(1):242–8. [PubMed: 10903925]
41. Mentlein R, Held-Feindt J. Pleiotrophin, an angiogenic and mitogenic growth factor, is expressed in human gliomas. *J Neurochem.* 2002; 83(4):747–53. [PubMed: 12421346]
42. Li YS, Milner PG, Chauhan AK, Watson MA, Hoffman RM, Kodner CM, et al. Cloning and expression of a developmentally regulated protein that induces mitogenic and neurite outgrowth activity. *Science.* 1990; 250(4988):1690–4. [PubMed: 2270483]
43. Tsutsui J, Uehara K, Kadomatsu K, Matsubara S, Muramatsu T. A new family of heparin-binding factors: strong conservation of midkine (MK) sequences between the human and the mouse. *Biochem Biophys Res Commun.* 1991; 176(2):792–7. [PubMed: 2025291]
44. Kuboyama K, Fujikawa A, Suzuki R, Noda M. Inactivation of Protein Tyrosine Phosphatase Receptor Type Z by Pleiotrophin Promotes Remyelination through Activation of Differentiation of Oligodendrocyte Precursor Cells. *J Neurosci.* 2015; 35(35):12162–71. [PubMed: 26338327]
45. Courty J, Dauchel MC, Caruelle D, Perderiset M, Barritault D. Mitogenic properties of a new endothelial cell growth factor related to pleiotrophin. *Biochem Biophys Res Commun.* 1991; 180(1):145–51. [PubMed: 1819274]
46. Kong Y, Bai PS, Nan KJ, Sun H, Chen NZ, Qi XG. Pleiotrophin is a potential colorectal cancer prognostic factor that promotes VEGF expression and induces angiogenesis in colorectal cancer. *Int J Colorectal Dis.* 2012; 27(3):287–98. [PubMed: 22065111]
47. Chauhan AK, Li YS, Deuel TF. Pleiotrophin transforms NIH 3T3 cells and induces tumors in nude mice. *Proc Natl Acad Sci U S A.* 1993; 90(2):679–82. [PubMed: 8421705]
48. Besse S, Comte R, Frechault S, Courty J, Joel de L, Delbe J. Pleiotrophin promotes capillary-like sprouting from senescent aortic rings. *Cytokine.* 2013; 62(1):44–7. [PubMed: 23481101]
49. Zhang N, Zhong R, Perez-Pinera P, Herradon G, Ezquerro L, Wang ZY, et al. Identification of the angiogenesis signaling domain in pleiotrophin defines a mechanism of the angiogenic switch. *Biochem Biophys Res Commun.* 2006; 343(2):653–8. [PubMed: 16554021]
50. Koch S, Tugues S, Li X, Gualandi L, Claesson-Welsh L. Signal transduction by vascular endothelial growth factor receptors. *Biochem J.* 2011; 437(2):169–83. [PubMed: 21711246]
51. Ramos JW. The regulation of extracellular signal-regulated kinase (ERK) in mammalian cells. *Int J Biochem Cell Biol.* 2008; 40(12):2707–19. [PubMed: 18562239]

52. Hu L, Wang J, Wang Y, Xu H. An integrin alphavbeta3 antagonistic modified peptide inhibits tumor growth through inhibition of the ERK and AKT signaling pathways. *Oncol Rep.* 2016; 36(4):1953–62. [PubMed: 27499314]
53. Eishingdrelo H, Kongsamut S. Minireview: Targeting GPCR Activated ERK Pathways for Drug Discovery. *Curr Chem Genom Transl Med.* 2013; 7:9–15. [PubMed: 24396730]
54. Keck PJ, Hauser SD, Krivi G, Sanzo K, Warren T, Feder J, et al. Vascular permeability factor, an endothelial cell mitogen related to PDGF. *Science.* 1989; 246(4935):1309–12. [PubMed: 2479987]
55. Leung DW, Cachianes G, Kuang WJ, Goeddel DV, Ferrara N. Vascular endothelial growth factor is a secreted angiogenic mitogen. *Science.* 1989; 246(4935):1306–9. [PubMed: 2479986]
56. Tokunaga CC, Mitton KP, Dailey W, Massoll C, Roumayah K, Guzman E, et al. Effects of anti-VEGF treatment on the recovery of the developing retina following oxygen-induced retinopathy. *Invest Ophthalmol Vis Sci.* 2014; 55(3):1884–92. [PubMed: 24550366]
57. Zhang L, Kundu S, Feenstra T, Li X, Jin C, Laaniste L, et al. Pleiotrophin promotes vascular abnormalization in gliomas and correlates with poor survival in patients with astrocytomas. *Sci Signal.* 2015; 8:ra125. [PubMed: 26645582]
58. Heroult M, Bernard-Pierrot I, Delbe J, Hama-Kourbali Y, Katsoris P, Barritault D, et al. Heparin affin regulatory peptide binds to vascular endothelial growth factor (VEGF) and inhibits VEGF-induced angiogenesis. *Oncogene.* 2004; 23(9):1745–53. [PubMed: 15001987]
59. Koutsoumpa M, Poimenidi E, Pantazaka E, Theodoropoulou C, Skoura A, Megalooikonomou V, et al. Receptor protein tyrosine phosphatase beta/zeta is a functional binding partner for vascular endothelial growth factor. *Mol Cancer.* 2015; 14:19. [PubMed: 25644401]
60. Papadimitriou E, Pantazaka E, Castana P, Tsaliou T, Polyzos A, Beis D. Pleiotrophin and its receptor protein tyrosine phosphatase beta/zeta as regulators of angiogenesis and cancer. *Biochim Biophys Acta.* 2016; 1866(2):252–65. [PubMed: 27693125]
61. Kokolakis G, Mikelis C, Papadimitriou E, Courty J, Karetsoy E, Katsoris P. Effect of heparin affin regulatory peptide on the expression of vascular endothelial growth factor receptors in endothelial cells. *In Vivo.* 2006; 20(5):629–35. [PubMed: 17091770]
62. Gerber HP, McMurtrey A, Kowalski J, Yan M, Keyt BA, Dixit V, et al. Vascular endothelial growth factor regulates endothelial cell survival through the phosphatidylinositol 3'-kinase/Akt signal transduction pathway. Requirement for Flk-1/KDR activation. *J Biol Chem.* 1998; 273(46):30336–43. [PubMed: 9804796]
63. Byeon SH, Lee SC, Choi SH, Lee HK, Lee JH, Chu YK, et al. Vascular endothelial growth factor as an autocrine survival factor for retinal pigment epithelial cells under oxidative stress via the VEGF-R2/PI3K/Akt. *Invest Ophthalmol Vis Sci.* 2010; 51(2):1190–7. [PubMed: 19834034]
64. Rosenstein JM, Mani N, Khaibullina A, Krum JM. Neurotrophic effects of vascular endothelial growth factor on organotypic cortical explants and primary cortical neurons. *J Neurosci.* 2003; 23(35):11036–44. [PubMed: 14657160]
65. LeBlanc ME, Wang W, Chen X, Caberoy NB, Guo F, Shen C, et al. Secretogranin III as a disease-associated ligand for antiangiogenic therapy of diabetic retinopathy. *J Exp Med.* 2017; 214(4):1029–47. [PubMed: 28330905]
66. Lynn KD, Roland CL, Brekken RA. VEGF and pleiotrophin modulate the immune profile of breast cancer. *Cancers (Basel).* 2010; 2(2):970–88. [PubMed: 24281102]

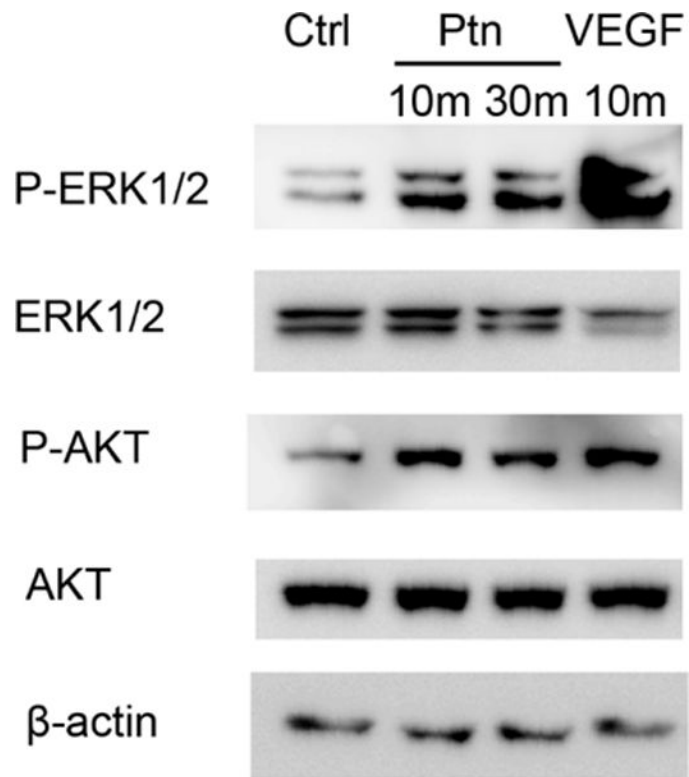


**Fig. 1.**

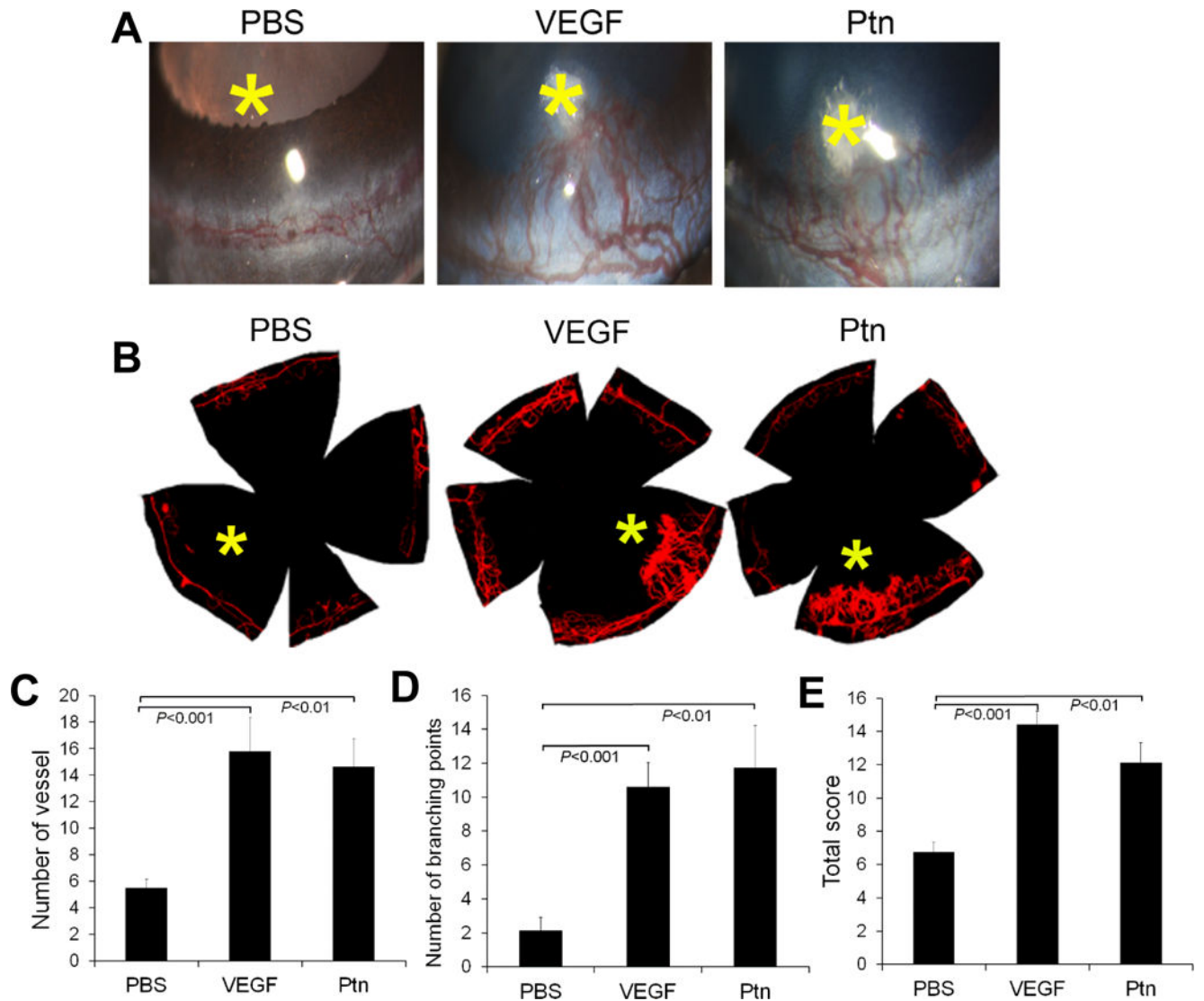
In vitro functional analyses of Ptn. **a** Ptn induces endothelial proliferation. HRMVECs were incubated with Ptn, VEGF or PBS control for 48 h in 96-well plates and quantified.  $n = 8$  wells. **b, c** Ptn promotes endothelial migration by wound healing assay. **b** Representative images of endothelial migration. HRMVECs were incubated with Ptn (200 ng/ml), VEGF (50 ng/ml) or PBS for 20 h. Bar 50  $\mu\text{m}$ . **c** The percentage of the denuded area covered by migrated cells within the original scratch was quantified.  $n = 3$  wells. **d, e** Ptn enhances HRMVEC migration in transwell assay. **d** Representative images of transwell migration assay with HRMVECs (DAPI signal). Ptn (200 ng/ml), VEGF (50 ng/ml) or PBS was in the bottom chamber for 8 h. Bar 50  $\mu\text{m}$ . **e**, Quantification of migrated cells/well.  $n = 4$  well. These assays were independently performed three times with similar outcomes. One representative experiment is shown.  $\pm$ SEM, \* $p < 0.05$ , \*\* $p < 0.01$ , \*\*\* $p < 0.001$ , versus control,  $t$  test.



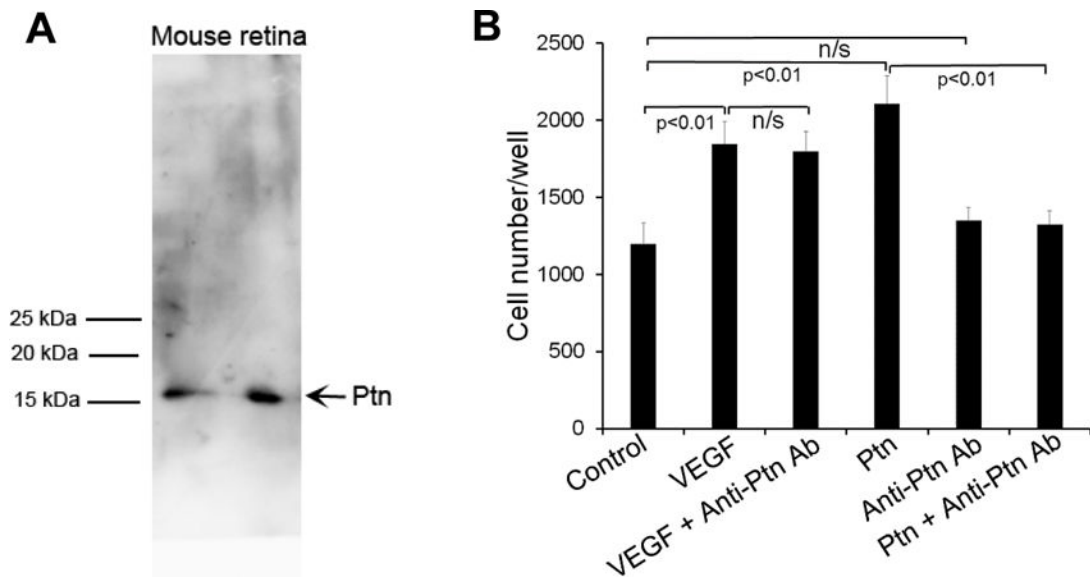
**Fig. 2.** Ptn stimulates spheroid sprouting of HRMVECs. **a** Representative images of spheroid sprouting. Ptn, 20 ng/ml; VEGF, 5 ng/ml. Bar 100 µl. **b** Quantification of endothelial sprouts. The average length of sprouts per spheroid was quantified. The assay was independently performed three times with similar outcomes. One representative experiment is shown.  $n = 7$  wells.  $\pm$ SEM, \*\*\* $p < 0.001$ , \*\*\*\* $p < 0.0001$ , versus control,  $t$  test.



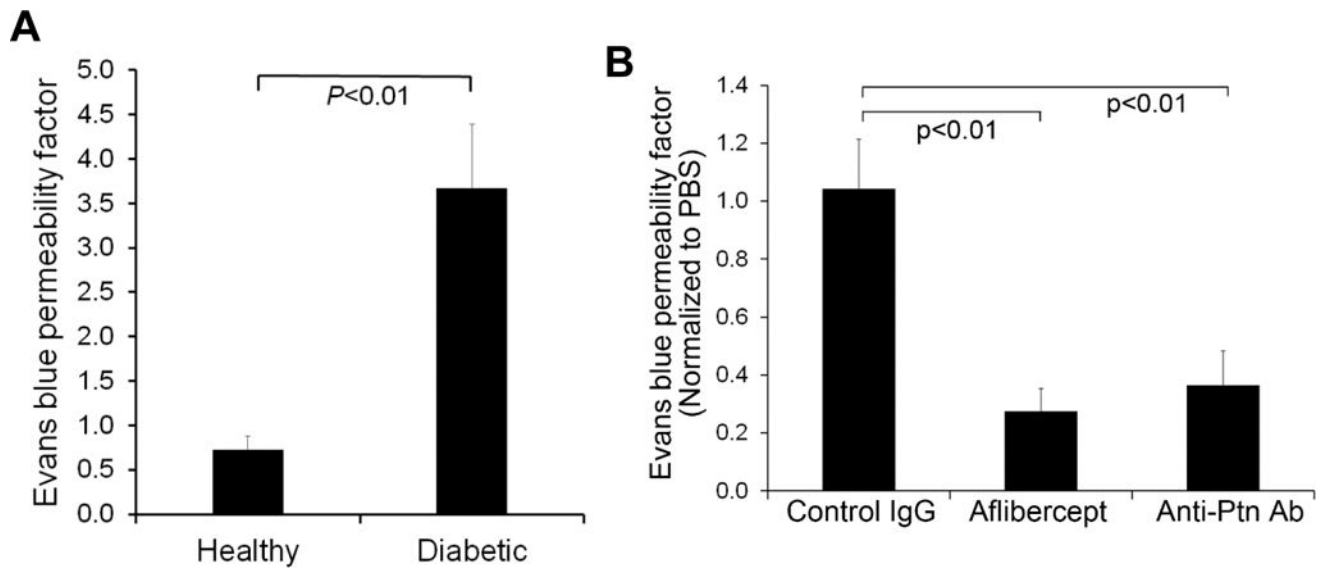
**Fig. 3.** Ptn activates ERK1/2 and Akt. HRMVECs were incubated with Ptn (200 ng/ml), VEGF (100 ng/ml) or PBS for 10 or 30 min. Phosphorylated and total ERK1/2 or Akt were detected by Western blot. These results were validated three times with similar outcomes.



**Fig. 4.** Ptn stimulates corneal angiogenesis. **a** Representative images of corneal angiogenesis by slit-lamp photography. Small pieces of filter papers presoaked in Ptn (250 ng/ml), VEGF (100 ng/ml) or PBS were implanted in corneal pockets to induce vascular growth for 6 days. Asterisk indicates filter paper position. **b** Representative images of corneal blood vessels labeled with fluorescent DiI dye. **c–e** Quantification of corneal angiogenesis. The numbers of new sprouting vessels into the cornea, branching points of corneal vessels and total new vessel score were quantified in **c–e**.  $n = 8$  corneas for Ptn, 5 for VEGF and 8 for PBS.  $\pm$ SEM, one-way ANOVA test.

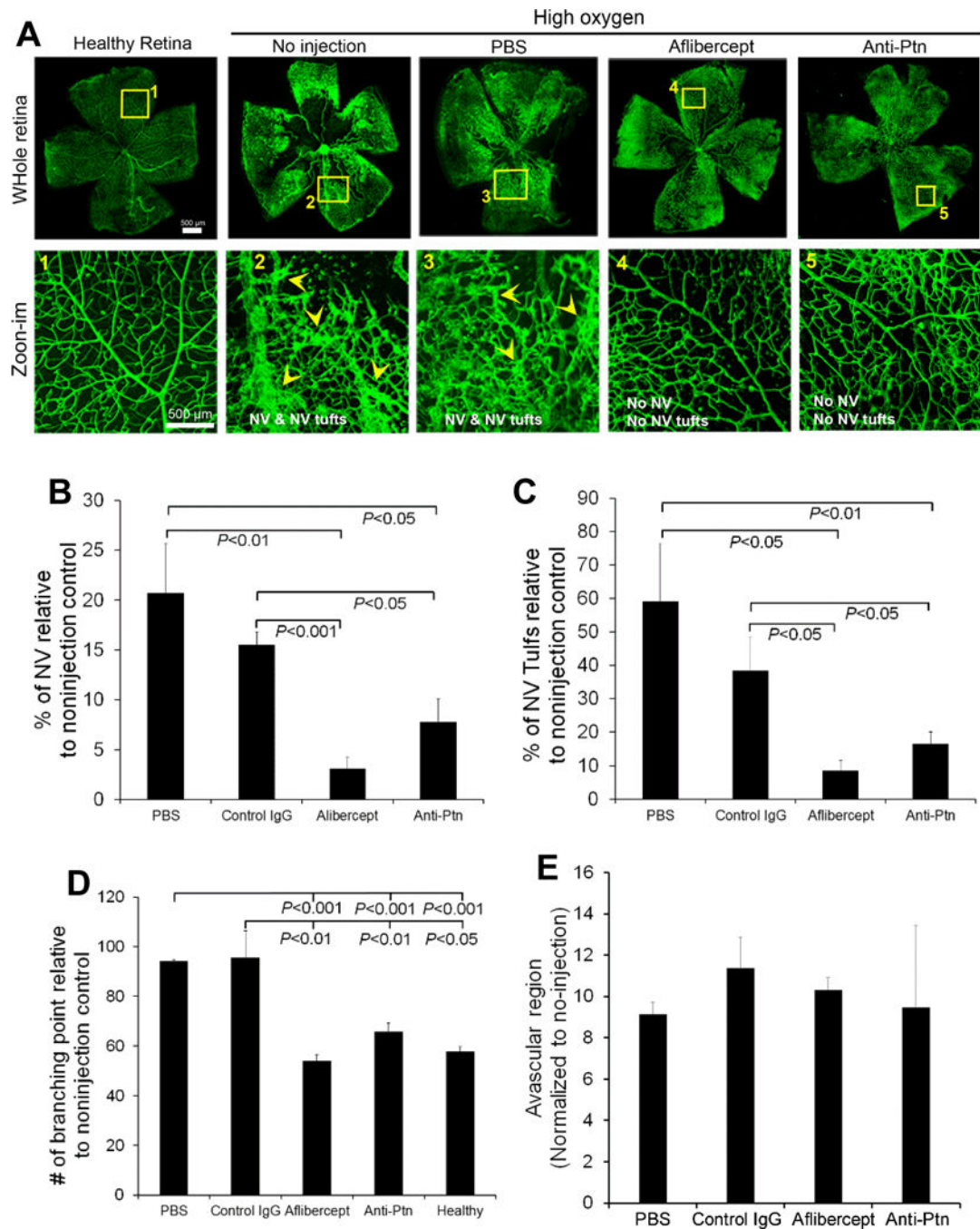


**Fig. 5.** Anti-Ptn Ab neutralizes Ptn-induced endothelial proliferation. **a** Affinity-purified anti-Ptn Ab specifically recognizes Ptn in mouse retinal homogenate. ~200  $\mu$ g/lane. **b** Proliferation assay with HRMVECs was performed as described in Fig. 1a. Ptn, 200 ng/ml; VEGF, 100 ng/ml; anti-Ptn Ab, 400 ng/ml. The assay was independently performed three times with similar outcomes. One representative experiment is shown.  $n = 8$  wells.  $\pm$ SEM, one-way ANOVA test.

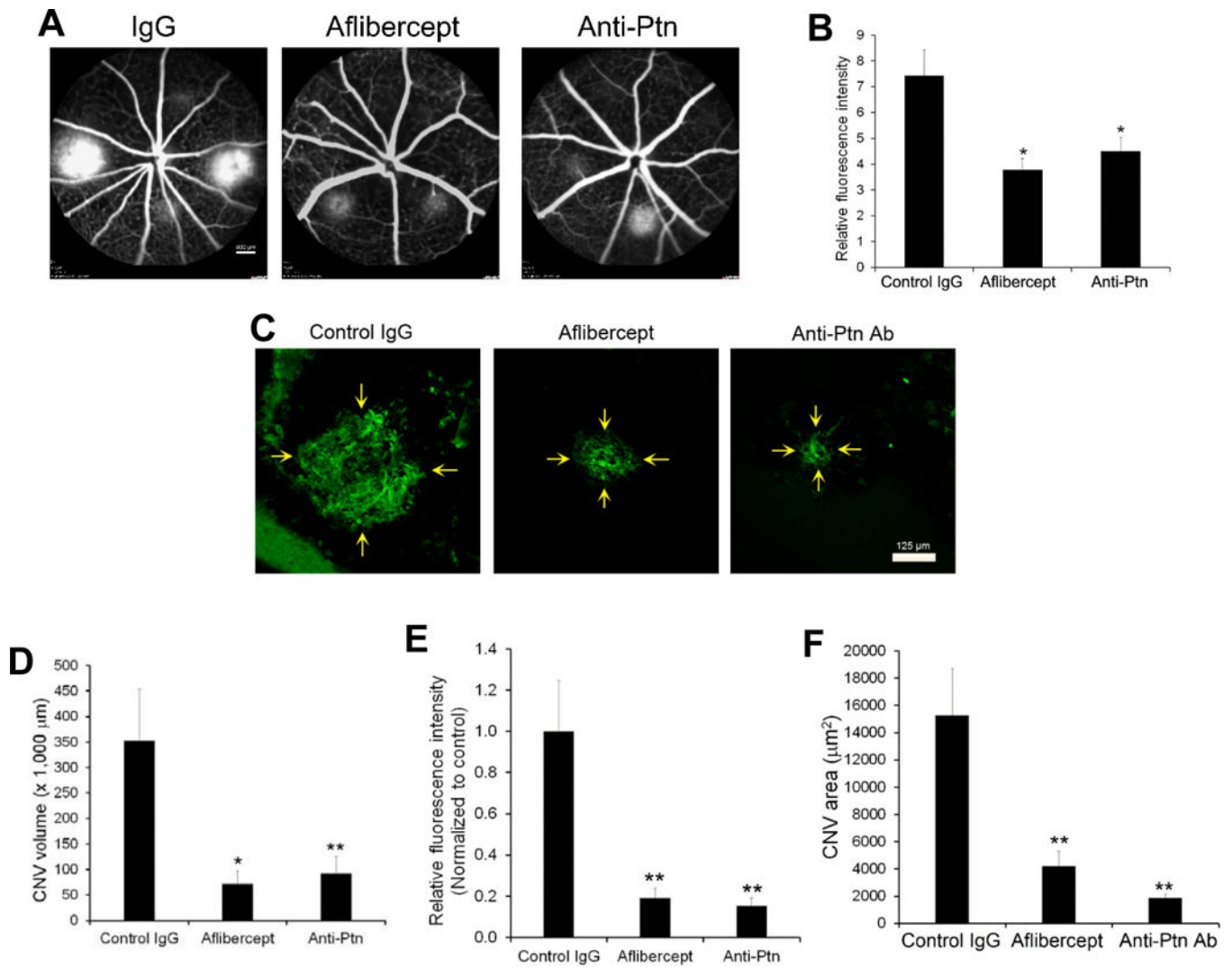


**Fig. 6.** Anti-Ptn Ab alleviates retinal vascular leakage in diabetic mice. **a** Retinal vascular leakage in 4-month-diabetic mice. The leakage was quantified by Evan blue assay.  $n = 6$  eyes. **b** Anti-Ptn therapy of DR. Intravitreal injection of anti-Ptn Ab reduced diabetic retinal vascular leakage. Data were normalized against PBS in fellow eyes. Anti-Ptn Ab,  $1.28 \mu\text{g}/1 \mu\text{l}/\text{eye}$ ; aflibercept,  $2 \mu\text{g}/1 \mu\text{l}/\text{eye}$ ; control IgG,  $1.28 \mu\text{g}/1 \mu\text{l}/\text{eye}$ .  $n = 6$  eyes for anti-Ptn and 5 for aflibercept or control IgG.  $\pm$ SEM, one-way ANOVA test.





**Fig. 7.** Anti-Ptn Ab prevents OIR-induced pathological neovascularization. **A** Representative images of OIR. Anti-Ptn (0.1  $\mu\text{g}/1 \mu\text{l}/\text{eye}$ ), aflibercept (2  $\mu\text{g}/1 \mu\text{l}/\text{eye}$ ) or control IgG (0.1  $\mu\text{g}/1 \mu\text{l}/\text{eye}$ ) was intravitreally injected at P12. RNV was analyzed at P17. Arrowheads indicate neovascularization (NV) and NV tufts. Bar 500  $\mu\text{m}$ . **b** Quantification of NV. **c** Quantification of NV tufts. **d** Quantification of branching points. **e** Quantification of avascular area in central retina.  $n = 11$  eyes for anti-Ptn, 4 for aflibercept, 6 for control IgG, 4 for PBS and 8 for healthy control.  $\pm$ SEM, one-way ANOVA test

**Fig. 8.**

Anti-Ptn Ab ameliorates laser-induced CNV. Mice were treated intravitreally with anti-Ptn ( $0.36 \mu\text{g}/1 \mu\text{l}/\text{eye}$ ), aflibercept ( $2 \mu\text{g}/1 \mu\text{l}/\text{eye}$ ) or control IgG ( $0.36 \mu\text{g}/1 \mu\text{l}/\text{eye}$ ) 3 days after laser photocoagulation. Fluorescein angiography was performed on Day 7. Eyecups without the retina were isolated from euthanized mice on Day 8, labeled with Alexa Fluor 488-isolectin B4, flat mounted and analyzed by confocal microscopy to detect CNV. **a** Representative images of fluorescein angiography. Bar  $800 \mu\text{m}$ . **b** Quantification of fluorescence intensity in **a**. **c** Representative images of Alexa Fluor 488-isolectin B4-labeled CNV. Bar  $125 \mu\text{m}$ . **d** Quantification of CNV 3D volume in **c**. **e** Quantification of CNV vessel density (i.e., fluorescence intensity) in **c**. **f** Quantification of CNV area size in **c**.  $n = 16$  laser spots for anti-Ptn, 22 for aflibercept and 22 for control IgG.  $\pm\text{SEM}$ , \* $p < 0.05$ , \*\* $p < 0.01$ , versus control IgG, one-way ANOVA test.